

2009

LINEAR COEFFICIENT OF THERMAL EXPANSION OF POROUS ANODIC ALUMINA THIN FILMS FROM ATOMIC FORCE MICROSCOPY

Richard X. Zhang

Purdue University - Main Campus

Timothy Fisher

Purdue University - Main Campus, tsfisher@purdue.edu

Arvind Raman

Purdue University - Main Campus, raman@purdue.edu

Timothy D. Sands

Purdue University - Main Campus, tsands@purdue.edu

Follow this and additional works at: <http://docs.lib.purdue.edu/nanopub>



Part of the [Nanoscience and Nanotechnology Commons](#)

Zhang, Richard X.; Fisher, Timothy; Raman, Arvind; and Sands, Timothy D., "LINEAR COEFFICIENT OF THERMAL EXPANSION OF POROUS ANODIC ALUMINA THIN FILMS FROM ATOMIC FORCE MICROSCOPY" (2009). *Birck and NCN Publications*. Paper 463.

<http://docs.lib.purdue.edu/nanopub/463>

This document has been made available through Purdue e-Pubs, a service of the Purdue University Libraries. Please contact epubs@purdue.edu for additional information.

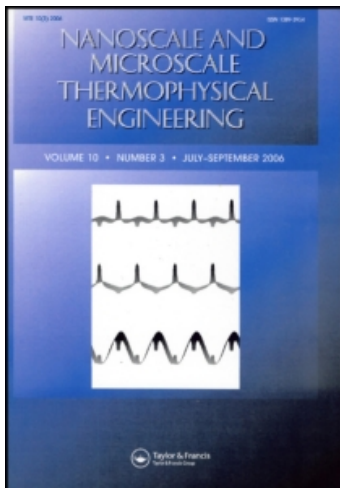
This article was downloaded by: [Purdue University]

On: 18 March 2010

Access details: Access Details: [subscription number 910629178]

Publisher Taylor & Francis

Informa Ltd Registered in England and Wales Registered Number: 1072954 Registered office: Mortimer House, 37-41 Mortimer Street, London W1T 3JH, UK



Nanoscale and Microscale Thermophysical Engineering

Publication details, including instructions for authors and subscription information:

<http://www.informaworld.com/smpp/title~content=t713774103>

Linear Coefficient of Thermal Expansion of Porous Anodic Alumina Thin Films from Atomic Force Microscopy

X. Richard Zhang ^a; T. S. Fisher ^a; A. Raman ^a; T. D. Sands ^b

^a School of Mechanical Engineering, School of Electrical & Computer Engineering, Birck

Nanotechnology Center, Purdue University, West Lafayette, Indiana, USA ^b School of Materials

Engineering, School of Electrical & Computer Engineering, Birck Nanotechnology Center, Purdue

University, West Lafayette, Indiana, USA

To cite this Article Zhang, X. Richard, Fisher, T. S., Raman, A. and Sands, T. D.(2009) 'Linear Coefficient of Thermal Expansion of Porous Anodic Alumina Thin Films from Atomic Force Microscopy', *Nanoscale and Microscale Thermophysical Engineering*, 13: 4, 243 – 252

To link to this Article: DOI: 10.1080/15567260903277039

URL: <http://dx.doi.org/10.1080/15567260903277039>

PLEASE SCROLL DOWN FOR ARTICLE

Full terms and conditions of use: <http://www.informaworld.com/terms-and-conditions-of-access.pdf>

This article may be used for research, teaching and private study purposes. Any substantial or systematic reproduction, re-distribution, re-selling, loan or sub-licensing, systematic supply or distribution in any form to anyone is expressly forbidden.

The publisher does not give any warranty express or implied or make any representation that the contents will be complete or accurate or up to date. The accuracy of any instructions, formulae and drug doses should be independently verified with primary sources. The publisher shall not be liable for any loss, actions, claims, proceedings, demand or costs or damages whatsoever or howsoever caused arising directly or indirectly in connection with or arising out of the use of this material.

LINEAR COEFFICIENT OF THERMAL EXPANSION OF POROUS ANODIC ALUMINA THIN FILMS FROM ATOMIC FORCE MICROSCOPY

X. Richard Zhang¹, T.S. Fisher¹, A. Raman¹, and T.D. Sands²

¹*School of Mechanical Engineering, School of Electrical & Computer Engineering, Birck Nanotechnology Center, Purdue University, West Lafayette, Indiana, USA*

²*School of Materials Engineering, School of Electrical & Computer Engineering, Birck Nanotechnology Center, Purdue University, West Lafayette, Indiana, USA*

In this article, a precise and convenient technique based on the atomic force microscope (AFM) is developed to measure the linear coefficient of thermal expansion of a porous anodic alumina thin film. A stage was used to heat the sample from room temperature up to 450 K. Thermal effects on AFM probes and different operation modes at elevated temperatures were also studied, and a silicon AFM probe in the tapping mode was chosen for the subsequent measurements due to its temperature insensitivity. The topography of the porous alumina sample was obtained, and the pore sizes and the surface roughness were analyzed. The thermal expansion of the sample was measured within the temperature range of 293 to 443 K. The results show that the linear coefficient of thermal expansion of the porous anodic alumina thin film is approximately two times larger than that of bulk alumina.

KEY WORDS: porous anaodic alumina, coefficient of thermal expansion, atomic force microscopy, thin films

INTRODUCTION

Porous anodic alumina (PAA) has been extensively studied over the past several decades. It has been demonstrated recently that a two-step anodization process can improve pore regularity with appropriate acid solutions [1, 2]. Highly ordered nanopore arrays can be fabricated inexpensively and reliably by this process, making PAA a useful template material for nanoscale fabrication. A variety of nanostructures, including nanowire arrays, carbon nanotubes, and nanopatterned DNA have been fabricated using PAA templates

Manuscript accepted 20 August 2009.

Support from the Multiscale Manufacturing Center at the School of Mechanical Engineering, Purdue University, is gratefully acknowledged. We also appreciate the help in preparing the PAA samples from Parijat Pramil Deb and Dr. Placidus Amama at the School of Materials Engineering and Matt Maschmann and Jun Xu at the School of Mechanical Engineering, Purdue University.

Current address for X. Richard Zhang: GE Global Research Center, Niskayuna, NY.

Address correspondence to A. Raman, School of Mechanical Engineering, School of Electrical & Computer Engineering, Birck Nanotechnology Center, Purdue University, West Lafayette, Indiana 47907. E-mail: raman@purdue.edu

[3–5]. In some of these applications where temperature changes occur, a coefficient of thermal expansion (CTE) mismatch exists between the PAA template and nanostructures inside the pores, and this mismatch may lead to reliability issues. However, little work has been done on linear CTE measurements of PAA thin films, primarily because of their small thickness and the extremely low total expansion along the thickness direction.

Traditional methods for measuring thermal expansion, such as push-rod dilatometers and optical interferometers, require large sample thickness (20–150 mm) [6]. X-ray diffraction has very high sensitivity but it is only appropriate for crystalline structures [7]. A number of techniques for measuring the linear CTE of thin films have been developed, such as the two-terminal capacitance method [8], optical beam lever [9, 10], ellipsometric technique [11], bilayer cantilever method [12], and atomic force microscopy (AFM)-based methods [13–15].

The AFM is a powerful tool in the study and characterization of materials at nanoscale dimensions because an AFM can provide not only qualitative but also quantitative information from the surface of virtually any material and is capable of measuring the thermal expansion of thin films due to its atomic resolution in the z-direction [16]. Scanning joule expansion microscopy (SJEM) [13] and scanning thermal expansion microscopy (STHEM) [15] have been developed to measure surface topography and material expansion simultaneously. An advantage of SJEM and STHEM is their high spatial resolution, which is about 10–50 nm, but both of these techniques require an external AC current source and a lock-in detector. In addition, the samples must be electrically conducting and metal microwires are usually used in SJEM and a special probe (Wollaston wire probe or microfabricated probe) is used in STHEM [15]. Therefore, these methods are not convenient if one wants to measure a nonconductive PAA film with conventional AFM probes.

In this article, we report a precise and convenient technique to perform linear CTE measurements of PAA with a commercial AFM (Veeco DI 3100, Veeco Inc., Santa Barbara, CA, USA) and a heated stage using tapping mode with a silicon AFM probe. The PAA was heated from room temperature to 450 K. Thermal expansion measurements at different temperatures were obtained by monitoring sample thickness changes, and the linear CTE was calculated afterwards.

EXPERIMENTS

A schematic of the experimental apparatus is shown in Figure 1. A DI 3100 AFM system, laser diode, piezo tube, and position sensitive detector (PSD) were all integrated together as a scanning head. This design provides spacious working room, which makes it possible to control temperature with a heated stage. The stage was mounted on an x–y sample stage, which has a large travel range (100 mm × 125 mm). The stage was made of brass, with dimensions of 50 mm × 25 mm × 12.5 mm (length × width × thickness). Two cartridge heaters (120 V, 100 Watt) were inserted inside it, and two thermocouples were buried directly under the top surface.

The PAA film was prepared using the standard two-step anodization. A 3- μm aluminum film was deposited on a glass substrate. The film was anodized first in a 0.5-M oxalic acid solution at 277 K under a constant voltage of 40 V for 40 min. After chemically removing the resultant aluminum oxide layer by immersing the sample in an aqueous mixture of phosphoric acid (5 wt%) and chromic acid (4 wt%) at 333 K for 10 min, a second anodization was performed under the same condition for 30 min.

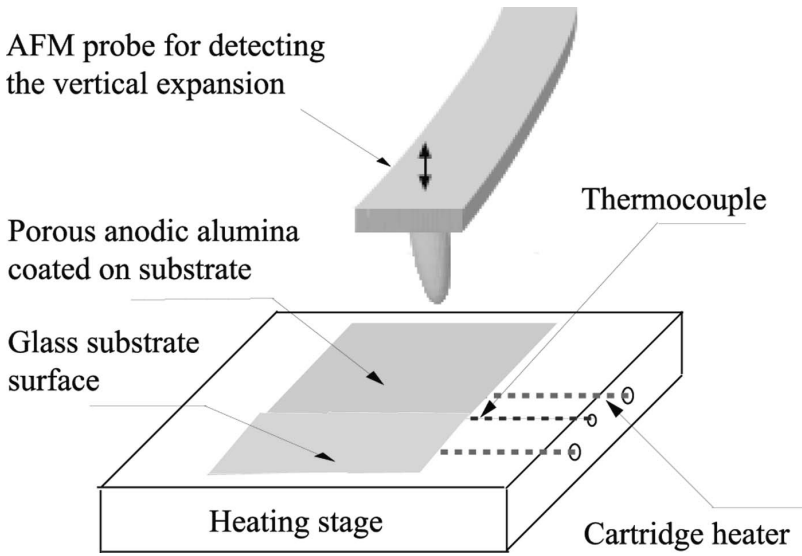


Figure 1. A schematic of the experimental apparatus for linear CTE measurements of PAA. When used in the tapping mode, the cantilever oscillation signals are passed through a lock-in amplifier, which provides the feedback variable for the scan.

During aluminum deposition, a mask was used to produce an uncoated area that was used as a reference for measuring the thickness of the PAA film.

Figure 2 shows an AFM topography image obtained in the tapping mode. A Veeco TESP probe was used at an operating frequency of 297 kHz. The scan area was

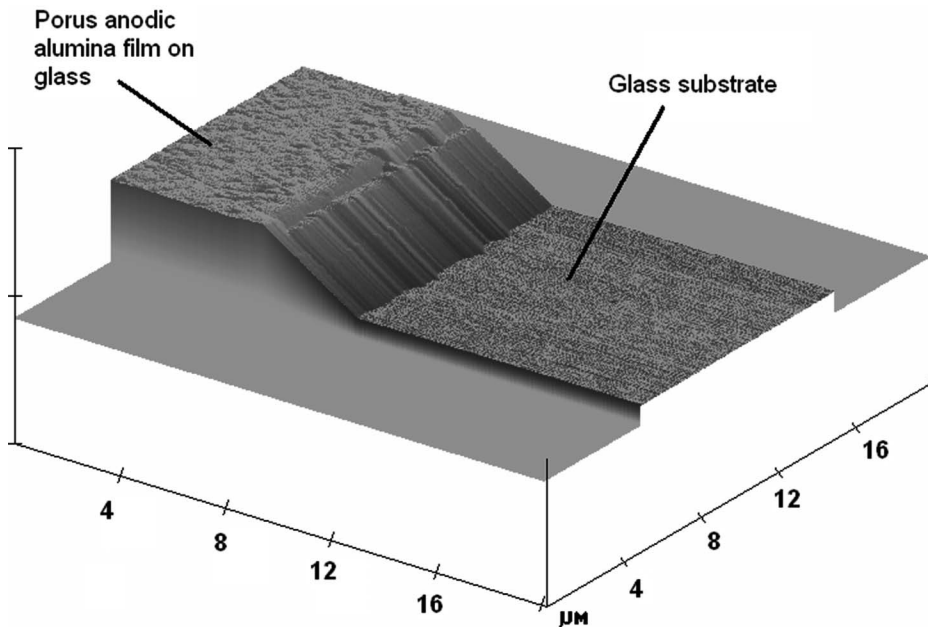


Figure 2. 3-D AFM topographic image of a PAA film on a glass substrate (scan size = 20 μm \times 10 μm).

20 $\mu\text{m} \times 10 \mu\text{m}$ and included both PAA and reference regions. The initial thickness of the PAA film, L_0 , can be obtained by comparing the height difference of the PAA and the glass using statistical depth analysis software (NanoscopeIIIa, Veeco Inc., Santa Barbara, CA, USA). After four scans were performed continuously over the same region at room temperature (T_0), the PAA film was heated by applying a voltage to the stage. During heating, the probe was withdrawn and kept approximately 700 μm away from the sample surface. Approximately 2 h were required to reach steady-state temperature (T_1) with a temperature fluctuation less than 0.2 K. The cantilever was returned to its resonant frequency at T_1 , and then the probe was engaged again with the same operating set point. Once engaged, approximately 20 min was needed to allow the AFM probe and the sample to reach thermal equilibrium. Then the sample height images were acquired over the same region for another four trials (each trial required approximately 4 min). The PAA film thickness change (ΔL) was then calculated. The same procedure was then repeated at higher temperatures.

THERMAL EFFECTS ON AFM PROBES

Performing AFM measurements at elevated temperatures is always challenging due to the thermal effects on AFM components, such as the probe, photodiode detector, and piezo tube. Probe bending (contact mode) and resonant frequency changes (tapping mode) are two important thermal effects.

In the contact mode, the tip of the AFM cantilever continuously touches the sample surface. Therefore, the cantilever heats up during scanning. Commonly used gold-coated silicon nitride cantilevers are known to be very sensitive to temperature changes [17]. A temperature change produces cantilever bending due to the thermal expansion difference of the two cantilever materials. To assess such effects in our AFM system, an experiment was performed using a contact mode cantilever (DNP-S, Veeco Inc., Santa Barbara, CA, USA). The distance between the cantilever tip and the PAA film was set to 700 μm . The temperature of the PAA film was increased from room temperature, and the corresponding change of voltage signal from the photodiode was recorded. The voltage signal represents the laser reflection from the back part of the cantilever and changes with the cantilever's vertical deflection. The experimental results, as plotted in Figure 3, show that the vertical voltage signal decreased with increasing temperature. The slope is approximately 3 nm/K after the voltage signal is converted into cantilever deflection. This result confirms the existence of thermal bending on the bimaterial contact mode cantilever. This phenomenon causes complications before and during probe scanning. Before scanning, one has to realign the laser beam on the photodiode to maintain the vertical signal value during heating. During scanning, tip-sample thermal equilibrium may be disturbed, and temperature fluctuations of 3 nm/K are too large for nanoscale thermal expansion measurements. Thus, we found that contact mode measurements with the bimaterial cantilever were not appropriate for our CTE measurement.

On the other hand, the thermal bending effect does not affect single-crystal tapping mode microcantilevers because uncoated silicon cantilevers are used. However, the resonant frequency of these cantilevers can shift when the cantilever is heated. The resonant frequency f_{res} of the first bending mode can be approximated by classical thin beam theory as

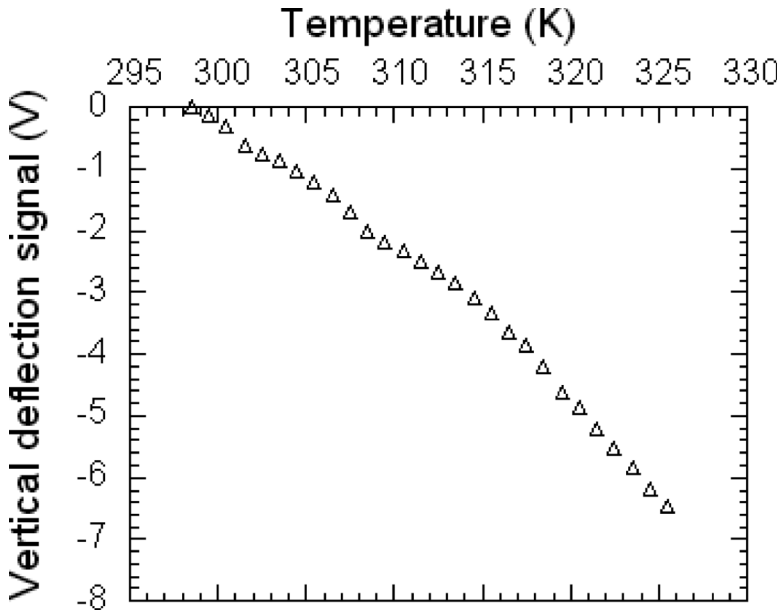


Figure 3. Temperature dependence of the vertical deflection of a gold-coated silicon nitride cantilever.

$$f_{res} = \frac{t}{2\pi l^2} \sqrt{\frac{E}{\rho}} \tag{1}$$

where t is the thickness of the cantilever and l is the length, E is the Young's modulus, and ρ is the density. The variation of f_{res} can be caused by the thermal expansion of the cantilever and the temperature dependence of the Young's modulus. Another experiment was performed to determine the dependence of the cantilever's resonant frequency on temperature. As shown in Figure 4, the resonant frequency decreases with the temperature almost linearly, and the slope is approximately 4.4 Hz/K. When the probe scans over the sample surface with a temperature variation of 1 K, the resonant frequency shifts by only 0.0015% for a cantilever with $f_{res} = 297.66$ kHz and is therefore negligible.

Based on the above study of thermal effects on AFM probes, the tapping mode operation with an uncoated silicon cantilever was chosen for PAA film CTE measurements. All of the following AFM images and measurements were taken using a Veeco TESP tapping mode probe with 297.66 kHz natural frequency.

RESULTS AND DISCUSSION

PAA Characterization

The PAA topography was obtained by AFM tapping mode with scan size of $2 \mu\text{m} \times 2 \mu\text{m}$. Figure 5 shows a surface image of the PAA film. The average pore size is

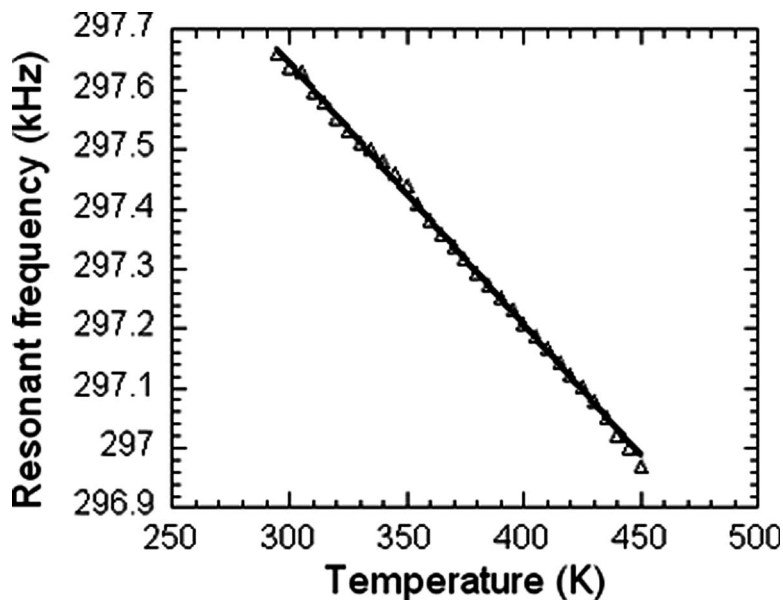


Figure 4. Temperature dependence of the resonant frequency of a silicon cantilever in tapping mode (solid line represents a linear fit to experimental data).

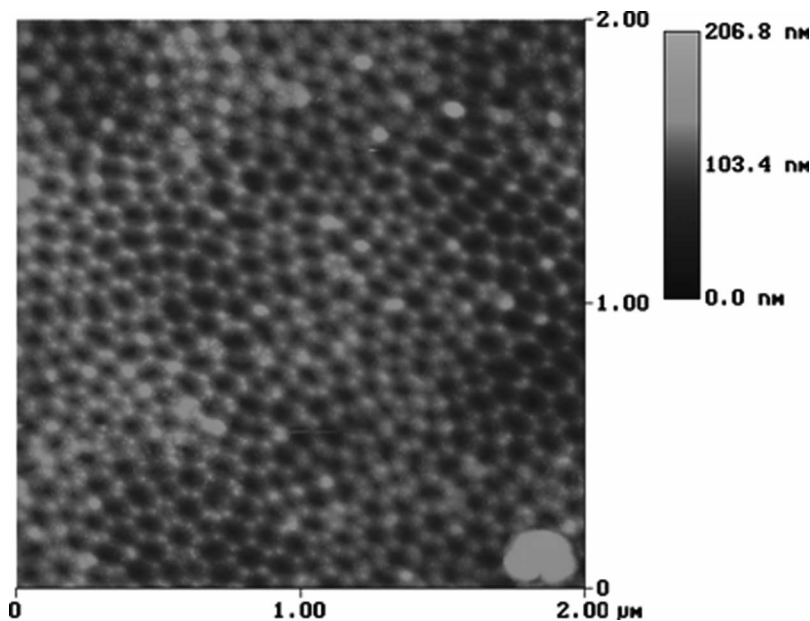


Figure 5. Surface image of the PAA film fabrication by two-step anodization.

estimated to be approximately 60 nm, which agrees with expectations based on anodization conditions. Roughness analysis was also performed by NanoscopeIIIa software. The root mean square roughness of the PAA surface was approximately 15 nm.

Linear CTE Measurement

After acquiring a complete AFM height image, the PAA film thickness can be measured. Although a single step height could have been measured by drawing a single line across the film, a more refined statistical approach was employed. Bearing analysis was provided by NanoscopeIIIa software to plot and analyze the distribution of surface height within a selected area. As shown in Figure 6a, a box with an area of $100 \mu\text{m}^2$ was selected in the AFM height image. The histograms of depth distribution within this box are shown in Figure 6b, where two peaks reveal two distinct levels of height of the PAA film and glass substrate. The PAA film thickness was determined by the distance between these two peaks. Four independent height images were captured, and thickness analysis was repeated three times for each image. The average thickness of the PAA film was $3.0822 \mu\text{m} \pm 0.6 \text{ nm}$ at room temperature ($T = 295.3 \text{ K}$).

The thickness of the PAA film was measured again at elevated temperatures, 345.6, 395.3, and 445.5 K. In each case the sample was preheated for several hours before the measurements were taken. Because PAA as prepared is nominally amorphous and hydrated, this step ensured that the PAA was dehydrated. Moreover, the increases in temperature were low enough that no crystallization of the PAA structure was likely to occur.

The changes of thickness with temperature, or absolute linear thermal expansions, are shown in Figure 7. A cubic function was applied to fit the experimental data. The fitting equation of linear thermal expansion $\Delta L/L_0$ over the range 295.3 K to 445.5 K is

$$\Delta L/L_0 = -1.9633 \times 10^{-2} + 1.611 \times 10^{-4}T - 4.73 \times 10^{-7}T^2 + 5.162 \times 10^{-10}T^3 \quad (2)$$

where T is absolute temperature and L_0 is the PAA film thickness at 295.3 K. In general, there are two categories of linear CTE definition depending on whether the expansion relates to a temperature range (mean CTE) or a single temperature (true CTE). The mean CTE is significantly lower than the true CTE due to the curvature of the $\Delta L/L_0$ versus temperature plot [18]. The true CTE is calculated in this article in order to compare with existing experimental data.

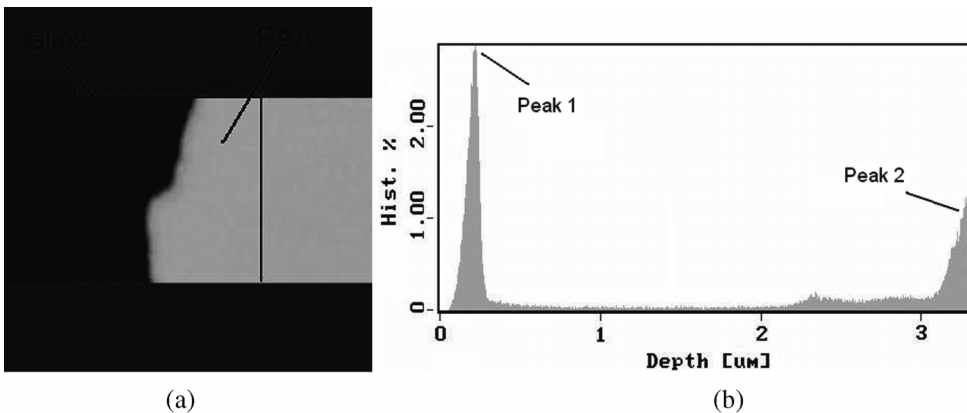


Figure 6. Bearing analysis of the PAA film thickness at $T = 295.3 \text{ K}$, (a) Height image, (b) histogram of depth distributions.

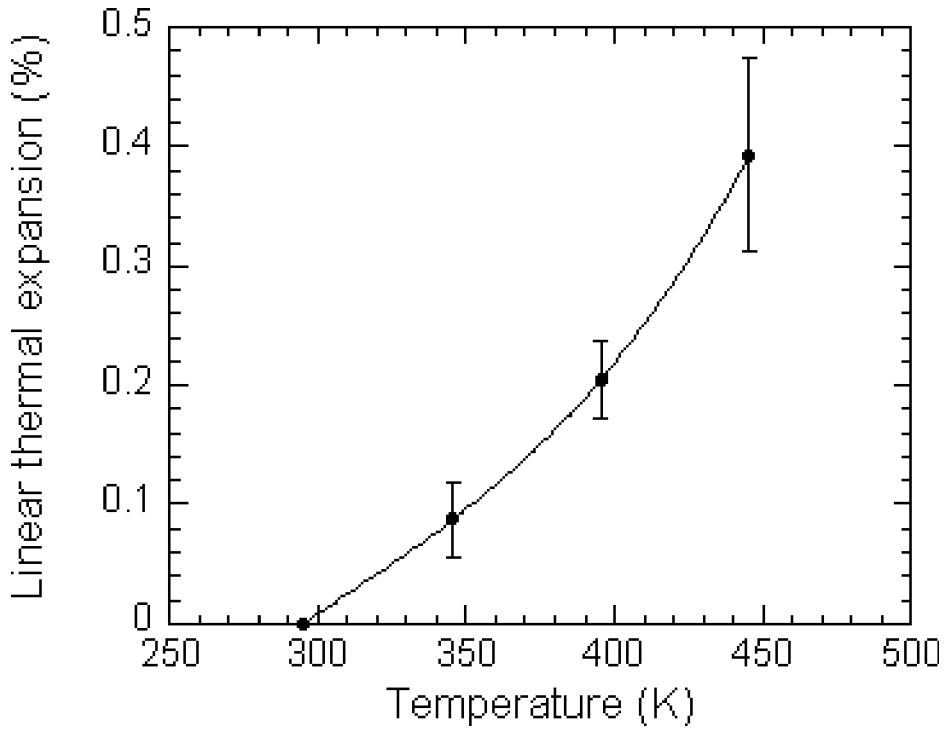


Figure 7. Linear thermal expansion of the PAA film at different temperatures.

From Eq. (2), the true linear CTE α can be obtained,

$$\alpha = \frac{1}{L_0} \frac{dL}{dT} = 1.611 \times 10^{-4} - 9.46 \times 10^{-7} T + 1.549 \times 10^{-9} T^2 \quad (295 - 445\text{K}) \quad (3)$$

Values derived from Eq. (3) are tabulated in Table 1. True linear CTE values of bulk alumina can be derived from experimental data [19] and are also listed in Table 1. It can be seen that the linear CTE of the PAA thin film is more than two times larger than that of bulk alumina. One possible reason is that the PAA is an anisotropic material and the dense nanopore structure of the PAA film enhances the linear thermal

Table 1 Values of true linear CTE of the PAA thin film and bulk alumina [6] at different temperatures

Temperature (K)	The true linear CTE (10^{-6} K^{-1})	
	PAA thin film	Bulk alumina
300	16.71	6.55
320	16.99	6.61
350	19.75	6.65
400	28.54	6.75

expansion of PAA film. Also, the CTE increases significantly at higher temperatures. This result may be an artifact produced by AFM components, such as the photodiode detector and piezo tube, which are temperature sensitive and need to be recalibrated at higher temperatures. Due to the above reasons, our technique was limited to the temperature range from room temperature to 400 K.

The technique described above assumes that no significant in-plane stresses are created during the heating of the PAA film, so that the expansion of the thickness can be attributed to unconstrained thermal expansion. In reality, the thin PAA film is a constrained elastic medium because it is bonded onto a glass substrate. Consequently, in-plane thermal stresses may develop in the film; these thermal stresses then affect, via the Poisson's ratio, the strain in the thickness direction. Moreover, because the thin film rests on a glass substrate, the in-plane thermal stresses may also generate bending moments near the edges of the thin film. To evaluate the above effects, a detailed 2-D finite element analysis was performed using isotropic elastic properties of bulk alumina and the linear CTE of bulk alumina. It was found that the thermal expansion of the film thickness upon heating from room temperature to 450 K was only 2% smaller if all above effects were considered. This indicates that for the temperature increases considered in the experiments, the in-plane thermal stresses are very small. Moreover, because the Poisson's ratio is small and thickness of the PAA is very small, the influence of these thermal stresses on the thermal expansion along the film thickness was minimal.

The minimum resolution of our thickness measurement was estimated to be 1 nm in the z-direction for this microscale film. The resolution in the z-direction is related to the sample thickness because of the nonlinearity of piezo tube, which is the critical component of the AFM scanner. Although a patented, nonlinear voltage waveform was applied to the piezo in our AFM system to increase linearity [20], we could only achieve a 1-nm z resolution for a 3- μm -thick film. We also studied thinner PAA films, with 200 nm and 1 μm thicknesses. However, while the piezo nonlinearity is mitigated, the thermal expansion is very small, leading to noisier CTE data.

CONCLUSION

We measured the linear coefficient of thermal expansion of a PAA thin film with a commercial AFM and a heated stage. No special AFM probes or external accessories were required in our technique. Two main AFM scanning modes—i.e., contact and tapping mode—were studied, and we conclude that an uncoated, silicon tapping mode probe is more appropriate for linear CTE measurements. The results indicate that the linear coefficient of thermal expansion of the PAA thin film is more than two times greater than that of bulk alumina.

REFERENCES

1. H. Masuda and K. Fukuda, Ordered Metal Nanohole Arrays Made by a Two-Step Replication of Honeycomb Structures of Anodic Alumina, *Science*, vol. 268, pp. 1466–1468, 1995.
2. H. Masuda, F. Hasegawa, and S. Ono, Self-Ordering of Cell Arrangement of Anodic Porous Alumina Formed in Sulfuric Acid Solution, *Journal of the Electrochemical Society*, vol. 144, pp. L127–L130, 1997.

3. M. Martin-Gonzalez, G.J. Snyder, A.L. Prieto, R. Gronsky, T. Sands, and A.M. Stacy, Direct Electrodeposition of Highly Dense 50 nm $\text{Bi}_2\text{Te}_{3-y}\text{Se}_y$ Nanowire Arrays, *Nano Letters*, vol. 3, pp. 973–977, 2003.
4. J.S. Suh and J.S. Lee, Highly Ordered Two-Dimensional Carbon Nanotube Arrays, *Applied Physics Letters*, vol. 75, pp. 2047–2049, 1999.
5. F. Matsumoto, M. Kamiyama, K. Nishio, and H. Masuda, Highly Ordered Nanopatterning of DNA with 40 nm Diameter Using Anodic Porous Alumina Substrate, *Japanese Journal of Applied Physics*, vol. 44, pp. L355–L358, 2005.
6. Y.S. Touloukian, R.K. Kirby, R.E. Taylor, and T.Y.R. Lee, *Thermophysical Properties of Matter: Vol. 13. Thermal Expansion-Nonmetallic Solids*, IFI/Plenum, New York, 1977.
7. D.N. Batchelder and R.O. Simmons, X-ray Lattice Constants of Crystals by a Rotating Camera Method: Al, Ar, Au, Cu, Ge, Ne, Si, *Journal of Applied Physics*, vol. 36, pp. 2864–2868, 1965.
8. H.V. Tiwary and G.D. Sao, An Electrical Method for the Measurement of Thermal Expansion of Thin Films, *Journal of Physics E: Scientific Instruments*, vol. 14, pp. 1378–1380, 1981.
9. D.S. Williams, Elastic Stiffness and Thermal Expansion Coefficient of Boron Nitride Films, *Journal of Applied Physics*, vol. 57, pp. 2340–2342, 1985.
10. B. Shi, W.J. Meng, and T.L. Daulton, Thermal Expansion of Ti-Containing Hydrogenated Amorphous Carbon Nanocomposite Thin Film, *Applied Physics Letters*, vol. 85, pp. 4352–4354, 2004.
11. H.R. Yuan, B.P. Hichwa, and T.H. Allen, Noncontact Method for Measuring Coefficient of Linear Thermal Expansion of Thin Films, *Journal of Vacuum Science and Technology A*, vol. 16, pp. 3119–3122, 1998.
12. W. Fang and C. Lo, On the Thermal Expansion Coefficients of Thin Films, *Sensors and Actuators*, vol. 80, pp. 310–314, 2000.
13. J. Varesi and A. Majumdar, Scanning Joule Expansion Microscopy at Nanometer Scales, *Applied Physics Letters*, vol. 72, pp. 37–39, 1998.
14. M. Igeta, T. Inoue, J. Varesi, and A. Majumdar, Thermal Expansion and Temperature Measurement in a Microscopic Scale by Using the Atomic Force Microscope, *JSME International Journal, Series B: Fluids and Thermal Engineering*, vol. 42, pp. 723–730, 1999.
15. A. Hammiche, D.M. Price, E. Dupas, G. Mills, A. Kulik, M. Reading, J.M.R. Weaver, and H.M. Pollock, Two New Microscopical Variants of Thermomechanical Modulation: Scanning Thermal Expansion Microscopy and Dynamic Localized Thermomechanical Analysis, *Journal of Microscopy*, vol. 199, pp. 180–190, 2000.
16. G. Binnig, C.F. Quate, and Ch. Gerber, Atomic Force Microscope, *Physical Review Letters*, vol. 56, pp. 930–933, 1986.
17. J. Lai, T. Perazzo, L. Shi, and A. Majumdar, Optimization and Performance of High-Resolution Micro-Optomechanical Thermal Sensors, *Sensors and Actuators A: Physical*, vol. 58, pp. 113–119, 1997.
18. J.D. James, J.A. Spittle, S.G.R. Brown, and R.W. Evans, A Review of Measurement Techniques for the Thermal Expansion Coefficient of Metals and Alloys at Elevated Temperatures, *Measurement Science and Technology*, vol. 12, pp. R1–R15, 2001.
19. Y.S. Touloukian, R.K. Kirby, R.E. Taylor, and T.Y.R. Lee, *Thermophysical Properties of Matter: Vol. 13. Thermal Expansion-Nonmetallic Solids*, IFI/Plenum, New York, 1977.
20. *Dimension 3100 Instruction Manual*, Veeco Inc., Santa Barbara, CA, USA, 2005.